

## Supporting Figure legends

### Figure S1. Testing dimedone switch method on low molecular weight and protein persulfides. Related to Figure 1.

- (A) Original Improved tag switch strategy for persulfide labeling.
- (B) ESI-TOF-MS spectrum of the reaction mixture containing 100  $\mu\text{M}$  nmc-penicillamine persulfide, 100  $\mu\text{M}$  NBF-Cl, and 500  $\mu\text{M}$  dimedone (ammonium carbonate buffer, pH 7.4, 23  $^{\circ}\text{C}$ ). 100  $\mu\text{M}$  nmc-penicillamine persulfide and 100  $\mu\text{M}$  NBF-Cl were mixed for 10 min and after the completion of the reaction dimedone was added and the reaction was monitored by ESI-TOF-MS. (C-E) Speciation of the observed (red) peaks and simulation of the isotopic distribution for each species (black).
- (F) MS/MS spectrum of  $m/z$  344 peak. Asterisk marks the position of  $m/z$  344 peak that decomposed to fragments which correspond to species shown in **Figure 1C**.
- (G) UV-vis spectral changes upon addition of 100  $\mu\text{M}$  NBF-Cl to 23  $\mu\text{M}$  HSA-SH (50 mM phosphate buffer, pH 7.4 with 1% SDS, at 37  $^{\circ}\text{C}$ ).
- (H) UV-vis spectral changes caused by subsequent addition of 100  $\mu\text{M}$  dimedone to the reaction mixture from (G). Inset: Kinetic trace at 420 nm.
- (I) UV-vis spectral changes upon addition of 100  $\mu\text{M}$  NBF-Cl to 23  $\mu\text{M}$  HSA-SOH (50 mM phosphate buffer, pH 7.4 with 1% SDS, at 37  $^{\circ}\text{C}$ ).
- (J) UV-vis spectral changes caused by subsequent addition of 100  $\mu\text{M}$  dimedone to the reaction mixture from (I). Inset: Kinetic trace at 420 nm.
- (K) UV-vis spectral changes upon addition of 100  $\mu\text{M}$  NBF-Cl to 23  $\mu\text{M}$  HSA-SSH (50 mM phosphate buffer, pH 7.4 with 1% SDS, at 37  $^{\circ}\text{C}$ ).

### Figure S2. Probing the selectivity and conditions for persulfide labeling by the Dimedone switch method. Related to Figure 2.

- (A) Human serum albumin (HSA), sulfenylated HSA and HSA persulfide were treated with 5 mM NBF-Cl (in 50 mM phosphate buffer, pH 7.4 with 1% SDS, at 37  $^{\circ}\text{C}$ ), precipitated and cleaned from NBF-Cl, and then incubated with 100  $\mu\text{M}$  DCP-Bio1 for 30 min at 37  $^{\circ}\text{C}$ . Following precipitation, proteins were resuspended in 50 mM phosphate buffer, pH 7.4 and spotted on a nitrocellulose membrane. Detection of dimedone-labeled adduct was done with streptavidin-Cy5. In addition, the same samples were incubated with streptavidin magnetic beads and after careful washing, the bound protein was eluted by boiling with Laemmli buffer for 5 min at 95  $^{\circ}\text{C}$ . Eluted proteins were separated by electrophoresis and in-gel fluorescence of NBF-protein adduct detected by Typhoon FLA 9500.
- (B) Detection of GAPDH and GAPDH-persulfide switch labeled with DCP-Bio1. Proteins were spotted on a nitrocellulose membrane and detection of dimedone-labeled (PSSH) adduct was done with streptavidin-Cy5. Green fluorescence (NBF-protein adduct) served as a measure of protein load.
- (C) MS/MS of peptide fragment obtained by trypsin digestion of bovine rhodanese (TST) shows labeling of C248 with hydrolyzed DCP-Bio1. Full MS data are given in Data S1-2.
- (D) Commercially available TST was either incubated with thiosulfate (TS) or DTT to form, the fully persulfidated or reduced form, respectively. 20  $\mu\text{M}$  enzyme was mixed with 50  $\mu\text{M}$  NBF-Cl and switch tagged for persulfide detection with DAz-2: Cy5 CuAAC. While both untreated and thiosulfate treated showed a Cy5 signal, the green fluorescence signal was significantly reduced in the fully persulfidated enzyme, despite having the same load. On the other hand, the green fluorescence signal was much stronger in the fully reduced enzyme, suggesting that at low NBF-Cl/protein ratio, switching caused by the dimedone-based probe could affect the intensity of green fluorescence. Top image: Coomassie Brilliant Blue (CBB, protein load); Middle image: 488 signal (NBF adduct); Bottom image: Cy5 image (persulfides).
- (E) 1 mM NBF-Cl (excess) was used to initially react with 20  $\mu\text{M}$  of TST, in an experiment similar to that shown in (D). The Cy5 signal was reduced when DTT treated TST was used, whilst the green fluorescence (488 nm) signal remained stable, suggesting that the green fluorescence can be used as a measure of the total protein load when excess NBF-Cl is used. It is worth mentioning that it is known that DTT is unable to fully reduce TST persulfide (Tandon and Horowitz, 1989). Top image: Coomassie Brilliant Blue (CBB, protein load); Middle image: green fluorescence signal (488, NBF adduct – protein load); Bottom image: Cy5 image (persulfides)
- (F) The reaction of HSA-SH with CuAAC reagents in all possible combinations (left) show no nonselective labeling. The same samples run 2 weeks after being kept at -20  $^{\circ}\text{C}$  show some small unselective labeling in the sample treated with Cy5-alkyne, Cu(II)-TBTA and ascorbate (due to the side reaction of alkynes with thiols – as a result of no NBF-

Cl used), but the signal was still negligible when compared to the signal obtained for fully labeled HSA-SSH. Top row: Cy5 signal; Middle row: 488 nm signal (NBF-adducts); Bottom row: Coomassie Brilliant Blue (CBB).

(G) Cyclic sulfenamides exist in equilibrium with sulfenic acids and react with NBF-Cl (Gupta and Carroll, 2016).

(H) Dimedone switch method efficiently distinguishes between protein sulfenic acid (and cyclic sulfenamide) and protein persulfides. PTP1B was used as a model system. Top row: Cy5 signal; Middle row: 488 nm signal (NBF-adducts); Bottom row: Coomassie Brilliant Blue.

(I) Depiction of experimental design used to test method's selectivity, shown in **Figure 2D**.

(J) In-gel detection of protein persulfidation levels (left; fire image) in HeLa cells, labeled with DAz-2/Cy5-alkyne CuAAC, with different concentrations of NBF-Cl. Green fluorescence (right) corresponds to NBF-protein adducts.

(K) Depiction of experimental design used to test method's cross reactivity with intracellular sulfenic acids and sulfenamides.

(L) Western blot of samples prepared by the protocol depicted in (K) is visualized by streptavidin Cy5. Blotting for vinculin was used as a loading control.

(M) Effect of dimedone pretreatment on persulfidation signal in MEF cells. Following steps depicted in (K), MEF cell lysates were labelled for protein persulfidation using DAz-2: Cy5 preclick mix. Bands were visualized using Typhoon 9500. Green signal corresponds to the protein load, and pseudocoloring with fire was used for PSSH signal.

**Figure S3. Broad applicability of dimedone switch method. Related to Figure 3.**

(A-B) Protein persulfidation levels (A) and corresponding CSE and CBS expression levels (B) in WT and CSE<sup>-/-</sup> cells of passage (P) 2 and 10. Green fluorescence (NBF adducts) used as a loading control for gels and GAPDH as a loading control for blots for normalization of signal.

(C) Confocal microscopy of *in situ* labeling of intracellular protein persulfidation. Negative control cells were incubated with DAz-2: Cy5 preclick mix prepared without DAz-2 (switching agent). CSE<sup>-/-</sup> MEF cells treated with 200  $\mu$ M Na<sub>2</sub>S (H<sub>2</sub>S) or 2 mM D-Cys for 1 hr. Cy5 signal corresponds to protein persulfides, 488 nm signal corresponds to NBF-adducts. Nuclei stained with DAPI. Scale bar 20  $\mu$ m. Related to the **Figure 3K**.

(D-F) High-resolution images of protein persulfidation in WT (D), CSE<sup>-/-</sup> (E) and WT MEF cells treated with D-Cys (2 mM, 1 hr) (F), obtained by wide-field fluorescence deconvolution. Scale bar 5  $\mu$ m.

(G) Protein evolution phylogenetic tree showing the common origin of cysteine containing MnSOD.

(H-I) MS/MS spectra of peptide obtained by chymotrypsin (H) and trypsin (I) digestion of persulfide labeled by Dimedone switch method (switch agent DCP-Bio1) MnSOD containing C193 labeled with hydrolyzed DCP-Bio1.

**Figure S4. Protein persulfidation is an integral part of the cellular response to H<sub>2</sub>O<sub>2</sub> and RTK activation. Related to Figures 4 and 5.**

(A) Representative blot showing the effect of GYY4137 (100  $\mu$ M, 30 min) on time-dependent H<sub>2</sub>O<sub>2</sub> (500  $\mu$ M)-induced sulfenylation in WT and CSE<sup>-/-</sup> MEF cells. Sulfenylation was labeled with DCP-Bio1 and visualized by streptavidin-488 and normalized to GAPDH. n = 3.

(B) Persulfidation, sulfenylation, sulfinylation and sulfonylation of DJ-1 in WT and CSE<sup>-/-</sup> MEF cells were treated with 100  $\mu$ M H<sub>2</sub>O<sub>2</sub> for 15 or 30 min. Samples for PSSH, PSOH and PSO<sub>2</sub>H were labeled using respective biotinylated reagents, immunoprecipitated with anti-DJ-1 antibody immobilized on agarose beads and immunoblotted against anti-biotin antibody. For sulfonylated DJ-1 (DJ-1-SO<sub>3</sub>H), an antibody selective for C106 DJ-1-SO<sub>3</sub>H was used. Related to **Figure 4E**.

(C) Expression levels of H<sub>2</sub>S producing enzymes, MST, CBS and CSE in HeLa cells after treatment with 100 ng/ml EGF for the indicated amount of time. Densitometric analysis of data from 3 independent experiments was normalized to  $\beta$ -tubulin. Values represent mean  $\pm$  SD. \* p < 0.05, \*\* p < 0.01 vs. 0 min.

(D-E) Representative images showing protein persulfidation and sulfenylation, used for **Figure 5C** and **5D** respectively. HeLa cells were pretreated with 100  $\mu$ M GYY4137 (30 min, D) or with 2 mM mixture of AOAA and PG (1:1, 30 min, E) and then exposed to 100 ng/ml EGF for the indicated amount of time. Persulfidation was detected in-gel by measuring Cy5/488 signal ratio. Sulfenylation was visualized by streptavidin-488 and normalized to  $\beta$ -tubulin. n = 3.

(F) Representative images showing protein persulfidation and sulfenylation, used for **Figure 5E**. HUVEC were treated with 40 ng/ml VEGF for the indicated amount of time. Persulfidation was detected in-gel by measuring Cy5/488 signal ratio. Sulfenylation was visualized by streptavidin-488 and normalized to  $\beta$ -tubulin. n=3.

(G) Representative images showing protein persulfidation used for **Figure 5F**. SH-SY5Y cells were treated with either 100 nM or 200 nM insulin for indicated time points. Persulfidation was detected in-gel by measuring Cy5/488 signal ratio. n = 3.

**(H)** Sulfenylation changes in SH-SY5Y cells treated with either 100 nM or 200 nM insulin for indicated time points. Sulfenylation was visualized by streptavidin-488 and normalized to GAPDH.  $n = 3$ . \*\*  $p < 0.01$  vs. 0 min.

**(I-J)** Changes in persulfidation and sulfenylation dynamics in WT and CSE<sup>-/-</sup> MEF cells after treatment with 100 ng/ml of EGF for indicated time points. Representative images **(I)** and quantification of the change **(J)**. Values are given as a mean  $\pm$  SD. from  $n = 3$ . \*  $p < 0.05$ , \*\*  $p < 0.01$  vs. 0 min.

**(K)** Inhibition of H<sub>2</sub>S production by the pretreatment of HeLa cells with 2 mM mixture of AOAA and PG (1:1, 30 min) and subsequent treatment with 100 ng/ml EGF for indicated time points causes changes in phosphorylation levels of pERK. Expression levels of pERK were normalized against total ERK expression in the same immunoblot, while total ERK was normalized to  $\beta$ -tubulin. Densitometric analysis of the data from 3 independent experiments is shown as a mean  $\pm$  SD. \*\*  $p < 0.01$  vs. control, <sup>#</sup>  $p < 0.01$  vs. same treatment in the control group.

**(L)** Antibody microarray-like approach was used to address persulfidation status of EGFR, PTEN, PTP1B and SHPTP2 from HeLa cells lysates treated with 100 ng/mL EGF for the indicated amount of time. Negative control represents wells where samples were added, but 5% BSA was added instead of an antibody. Original readouts obtained by Typhoon FLA 9500 are pseudo-coloured in ImageJ to visually enhance the changes in the signal (right). Quantification of the data from two independent experiments (left). \*  $p < 0.05$ , \*\*  $p < 0.01$ .

**(M-R)** Persulfidation levels of  $\beta$ -catenin **(M)**, actin **(N)**, E-cadherin **(O)**, Dok-2 **(P)**, VAV1 **(Q)**, RhoA **(R)** in HeLa cells lysates treated with or without 100 ng/ml EGF for 30 min and labeled for persulfides (switching agent DAz-2: Cy5), measured using EGFR pathway microarray glass slips. Related to **Figures 5J, K**. Each antibody was spotted in pentaplicates. Values are given as a mean  $\pm$  SD. from two independent experiments. \*  $p < 0.05$ , \*\*  $p < 0.01$  vs. control.

**Figure S5. Trx-catalyzed reduction of S-sulfocysteine (SSC) and protection against ROS-induced death. Related to Figure 6**

**(A)** Deconvoluted mass spectra of 10  $\mu$ M C32S Trx before (black) and after (red) the reaction with 10  $\mu$ M SSC showing no difference. Related to **Figure 6C**.

**(B)** ESI-TOF-mass spectra of 10  $\mu$ M C35S Trx before (black) and after the reaction with 10  $\mu$ M SSC (red). The arrow indicates the TrxS-S-Cys peak that is absent in the control spectrum. Related to **Figure 6D**.

**(C)** Kinetics of human Trx (4  $\mu$ M) oxidation with 25  $\mu$ M (blue line) and 50  $\mu$ M SSC (red line), followed by tryptophan fluorescence ( $\lambda_{ex}$  280 nm) changes. Spontaneous oxidation of Trx alone (Control) is shown in black.

**(D-E)** Activities of human Trx **(D)** with cystine (Cys<sub>2</sub>, black) or SSC (red) and, Trx1 (black) or TRP14 with SSC **(E)** where NADPH oxidation was recorded on a Tecan Infinite M200 plate reader, set to record absorption at 340 nm. 3  $\mu$ M human Trx1 or TRP14, 30 nM TrxR from rat liver and 250  $\mu$ M NADPH were used in all measurements. Concentration of cystine or SSC were set at 1 mM. The initial rate of A<sub>340</sub> decrease was fitted linearly, and consumption of NADPH over time was determined using an NADPH extinction coefficient  $\epsilon_{340}$  of 6020 M<sup>-1</sup> cm<sup>-1</sup>.

**(F)** Metabolic pathways for H<sub>2</sub>S biosynthesis in *S. cerevisiae*.

**(G)** Growth curves for BY4247 (WT),  $\Delta$ cys3 and  $\Delta$ cys4 mutants of *S. cerevisiae*. \*\*  $p < 0.01$  vs. WT.

**(H)** Persulfidation level in BY4247 (WT),  $\Delta$ cys3,  $\Delta$ cys4 and  $\Delta$ tum1 mutants of *S. cerevisiae*. Green fluorescence (488, NBF-adducts) was used as a loading control. Persulfidation was detected in-gel by measuring Cy5/488 signal ratio. Quantification of persulfidation levels in different mutants (right). Values represent mean  $\pm$  SD. \*\*  $p < 0.01$  vs. WT.

**(I)** Flow cytometric analysis of H<sub>2</sub>S levels (green fluorescence, FL1A) in BY4247 (WT) and the  $\Delta$ cys3 mutant of *S. cerevisiae*. Cells were incubated with 20  $\mu$ M MeRho-Az sensor (45 min, 30 °C). \*\*  $p < 0.01$  vs. WT.

**(J)** The effect of short-term (3 hr) pre-exposure to GYY4137 (500  $\mu$ M) or AP39 (100 nM) on the percentage of dead N2 *C. elegans* after 5 hr of 60 mM paraquat.  $n > 50$  worms. \*\*  $p < 0.01$  vs. untreated.

**(K)** The effect of short-term (3 hr) pre-exposure to GYY4137 (500  $\mu$ M) on the survival rate of N2 and *cth-1* mutant exposed to 5 mM sodium arsenite over 5 hr.  $n > 50$  worms. \*\*  $p < 0.01$  vs. untreated.

**Figure S6. PSSH levels correlate with aging. Related to Figure 7.**

**(A)** Lifespan analysis of N2, *cth-1* and *mpst-3* mutant strains.  $n > 110$  per line. N2 = 17.8 $\pm$ 0.5 days, *mpst-3* = 15.7 $\pm$ 0.4 days,  $p = 0.0003$ .

**(B)** Persulfidation levels in N2 *C. elegans* at different days of adulthood. Intensity of persulfidation is expressed as a Cy5/488 signal ratio. Values represent mean  $\pm$  SD. from  $n = 3$ . \*\*  $p < 0.01$  vs. Day 1.

**(C)** Expression levels of CSE, CBS and MPST in brain extracts from 1-, 6-, 12- and 24-month-old male Wistar rats. GAPDH is used as a loading control. Representative blots from  $n = 3$ .

**(D)** Persulfidation levels (left) and expression levels of CSE, CBS and MPST in liver extracts of 1-, 6-, 12- and 24-month-old male Wistar rats. Persulfidation was detected in-gel by measuring Cy5/488 signal ratio. GAPDH was used as a loading control for the expression levels. Representative images from  $n = 3$ .

(E) Expression levels of CSE, CBS and MPST in muscle extracts of 2- and 12-month-old male mice. GAPDH is used as a loading control. Densitometric analysis (right) of the data from 3 independent experiments is shown as a mean  $\pm$  SD. \*\*  $p < 0.01$  vs. 2 mo. Related to **Figure 7I**.

(F) Protein persulfidation levels in HeLa cell lysates, treated with or without thiosulfate (500  $\mu$ M) or thiosulfate sulfur transferase (TST, 5  $\mu$ M) or both, for 1 hr, 37 °C. Persulfidation was detected in-gel by measuring Cy5/488 signal ratio. Values represent mean  $\pm$  SD. \*\*  $p < 0.01$  vs. control.

**Table S1. List of proteins found to be endogenously persulfidated in human red blood cells.\*****Related to Figure 2.**

Nº	Protein name (UniProtKB database)	UniProtKB	-10logP	Peptides	Coverage %	MW (Da)	Modification/Ref.**
1	Carbonic anhydrase 1	P00915	308.61	54	73	28,870	PSX/(Delobel et al., 2016)
2	Spectrin alpha chain, erythrocytic 1	P02549	266.65	101	43	280,014	PSX/(Zaccarin et al., 2014)
3	Spectrin beta chain, erythrocytic	P11277	248.03	61	30	246,468	PSX/(Zaccarin et al., 2014)
4	Ankyrin 1	P16157	218.79	32	21	206,265	PSX/(Yang et al., 2012; Zaccarin et al., 2014)
5	Catalase	P04040	218.65	35	45	59,756	PSX/(Delobel et al., 2016; Yang et al., 2012)
6	Flavin reductase	P30043	197.55	17	64	22,119	PSX/(Delobel et al., 2016)
7	Band 3 anion transport protein	P02730	197.26	23	26	101,792	PSX/(Zaccarin et al., 2014)
8	Carbonic anhydrase 2	P00918	192.22	25	65	29,246	PSX/(Delobel et al., 2016)
9	Peroxiredoxin 2	P32119	187.35	26	59	21,892	PSX/(Delobel et al., 2016; Zaccarin et al., 2014)
10	Bisphosphoglycerate mutase	P07738	135.16	14	51	30,005	PSX/(Delobel et al., 2016)
11	Glyceraldehyde-3-phosphate dehydrogenase	P04406	131.26	9	39	36,053	PSX,PSSH/(Valentine et al., 1987; Zaccarin et al., 2014)
12	Protein/nucleic acid deglycase DJ-1	Q99497	129.49	8	50	19,891	PSX/(Delobel et al., 2016)
13	Peroxiredoxin 1	Q06830	123.63	10	45	22,110	PSX/(Delobel et al., 2016)
14	Protein DDI1 homolog 1	Q8WTU0	121.85	6	22	44,124	
15	Fructose-bisphosphate aldolase A	P04075	116.71	9	20	39,420	PSOH/(Valentine et al., 1987)
16	Purine nucleoside phosphorylase	P00491	114.54	7	30	32,118	PSX/(Delobel et al., 2016)
17	Methanethiol oxidase	Q13228	112.56	7	17	52,391	
18	Protein 4.1	P11171	112.26	7	10	97,017	PSX/(Yang et al., 2012; Zaccarin et al., 2014)
19	Transitional endoplasmic reticulum ATPase	P55072	164.3	16	21	89,322	PSX/(Yang et al., 2012)
20	Peroxiredoxin 6	P30041	153	11	52	25,035	PSX/(Delobel et al., 2016)
21	Stress-induced-phosphoprotein 1	P31948	140.13	11	19	62,639	PSX/(Delobel et al., 2016)
22	Triosephosphate isomerase	P60174	125.54	6	31	30,791	PSX/(Delobel et al., 2016)
23	Phosphoglycerate kinase 1	P00558	120.79	8	19	44,615	PSSH/(Valentine et al., 1987)

24	Heat shock cognate 71 kDa protein	P11142	119.28	10	20	70,898	PSX/(Delobel et al., 2016; Yang et al., 2012)
25	Tropomyosin alpha-3 chain	P06753	112.7	6	25	32,950	
26	L-lactate dehydrogenase B chain	P07195	111.71	10	25	36,638	PSX/(Delobel et al., 2016)
27	Alpha enolase	P06733	107.69	7	21	47,169	PSX, PSSH/ (Delobel et al., 2016; Valentine et al., 1987; Yang et al., 2012)
28	T-complex protein 1 subunit theta	P50990	106.44	7	16	59,621	
29	Low molecular weight phosphotyrosine protein phosphatase	P24666	103.76	5	38	18,042	
30	Alpha adducin	P35611	99.94	7	11	80,955	PSX/(Yang et al., 2012)
31	Erythrocyte band 7 integral membrane protein	P27105	98.78	7	29	31,731	PSX/(Zaccarin et al., 2014)
32	Eukaryotic translation initiation factor 5 alpha	P55010	95.91	4	31	49,223	
33	Heat shock protein HSP 90-alpha	P07900	94.83	7	13	84,660	
34	Peroxiredoxin 4	Q13162	93.27	6	11	30,540	
35	Adenylate kinase isoenzyme 1	P00568	91.30	5	23	21,635	PSSH/(Valentine et al., 1987)
36	Ubiquitin-like modifier-activating enzyme 1	Q5JRR6	89.97	4	5	56,852	PSX/(Yang et al., 2012)
37	Ubiquitin carboxyl-terminal hydrolase 14	P54578	87.61	4	13	56,069	PSX/(Yang et al., 2012)
38	$\beta$ adducin	P35612	87.23	3	5	80,854	
39	Hsc70 interacting protein	P50502	85.19	4	12	41,332	
40	Proteasome subunit alpha type-5	P28066	82.21	3	18	26,411	
41	Thioredoxin	P10599	79.82	4	31	11,737	
42	Rab GDP dissociation inhibitor $\beta$	P50395	79.5	4	10	50,663	PSX/(Delobel et al., 2016)
43	Glutathione S-transferase A1	P08263	78.34	3	13	25,631	PSX/(Delobel et al., 2016)
44	Erythrocyte membrane protein band 4.2	P16452	75.97	4	8	77,009	PSX/(Zaccarin et al., 2014)
45	Rho GDP dissociation inhibitor 1	P52565	75.91	3	16	23,207	
46	Dematin	Q08495	75.59	4	12	45,514	
47	Ankyrin 3	Q12955	75.45	5	1	480,410	PSX/(Zaccarin et al., 2014)
48	3-mercaptopyruvate sulfur transferase	P25325	68.09	4	9	33,178	
49	Carbonic anhydrase 3	P07451	69.76	3	14	29,557	PSX/(Delobel et al., 2016)
50	Ubiquitin conjugating enzyme E2	P51668	72.33	3	30	16,602	

51	Serine/threonine protein kinase OSR1	O95747	68.46	4	8	58,022	
52	Copper chaperone for superoxide dismutase	O14618	67.22	3	10	29,041	
53	Transaldolase	P37837	66.97	4	9	37,540	PSX/(Delobel et al., 2016)
54	Protein S100-A6	P06703	80.68	5	43	10,180	
55	Malate dehydrogenase	P40925	60.29	3	13	36,426	PSX/(Delobel et al., 2016)
56	Glutamate--cysteine ligase catalytic subunit	P48506	59.76	2	10	72,766	
57	Proteasome subunit alpha type-1	P25786	59.18	2	10	29,556	
58	14-3-3 protein beta/alpha	P31946	50.89	2	8	28,082	

\* The table consists of proteins identified by at least 2 reliable peptides and  $-10\log P > 50$ , obtained by trypsin and/or chymotrypsin digestion.

\*\*PSX denotes any kind of DTT-reducible cysteine oxidation (PSSH, PSOH, PSSP). PSSH denotes protein persulfidation specifically.

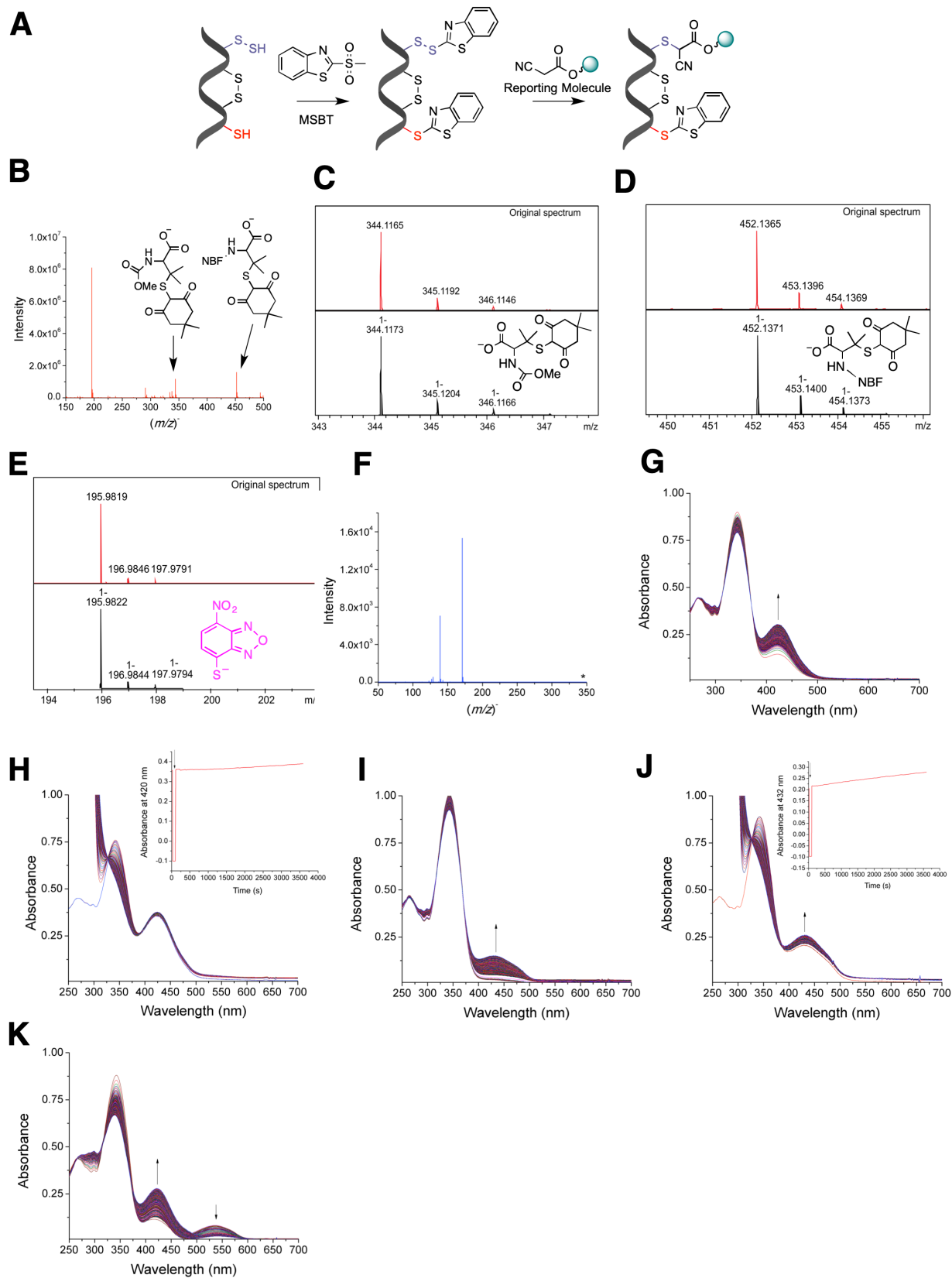


**Figure S1. Testing dimedone switch method on low molecular weight and protein persulfides. Related to Figure 1.**



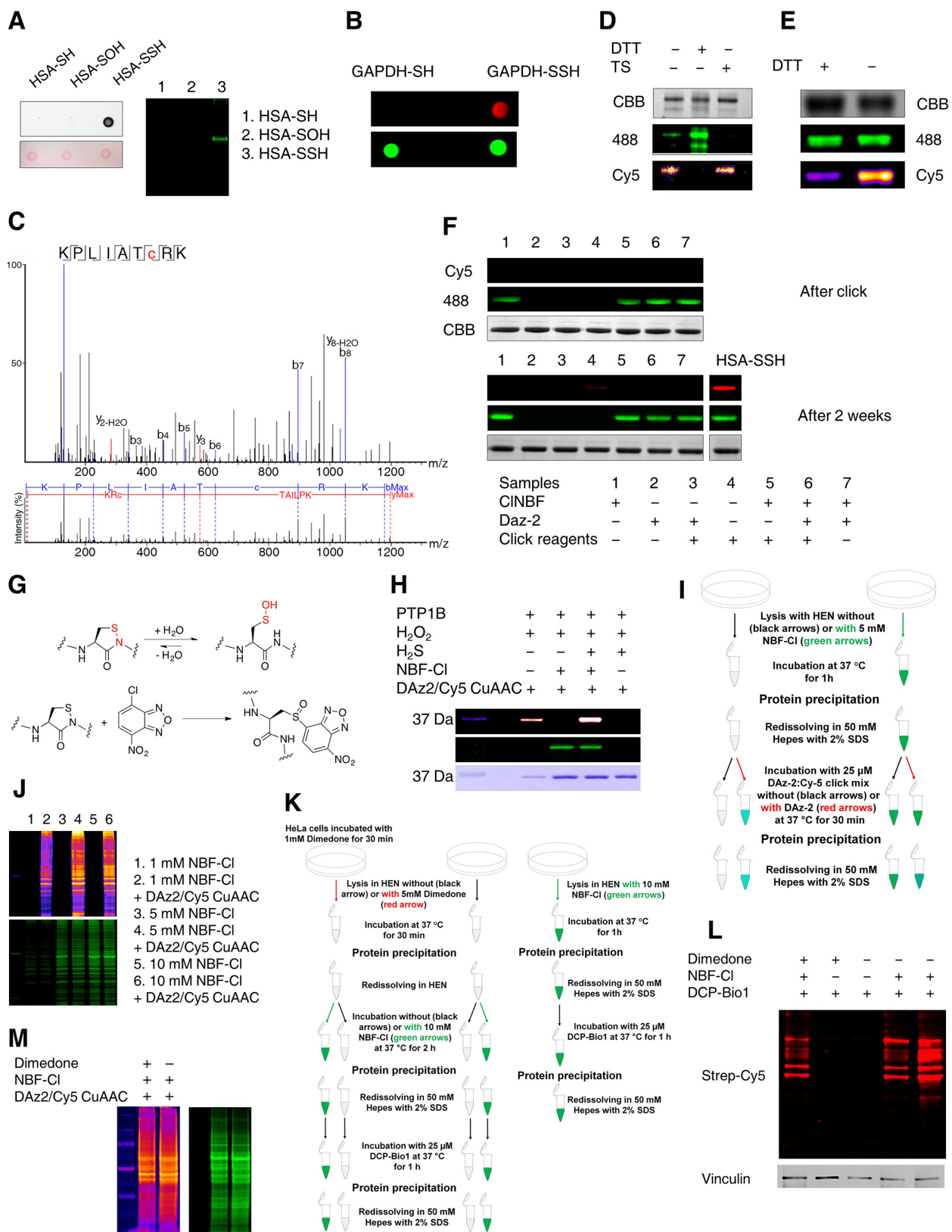


Figure S2. Probing the selectivity and conditions for persulfide labeling by the Dimedone switch method. Related to Figure 2.

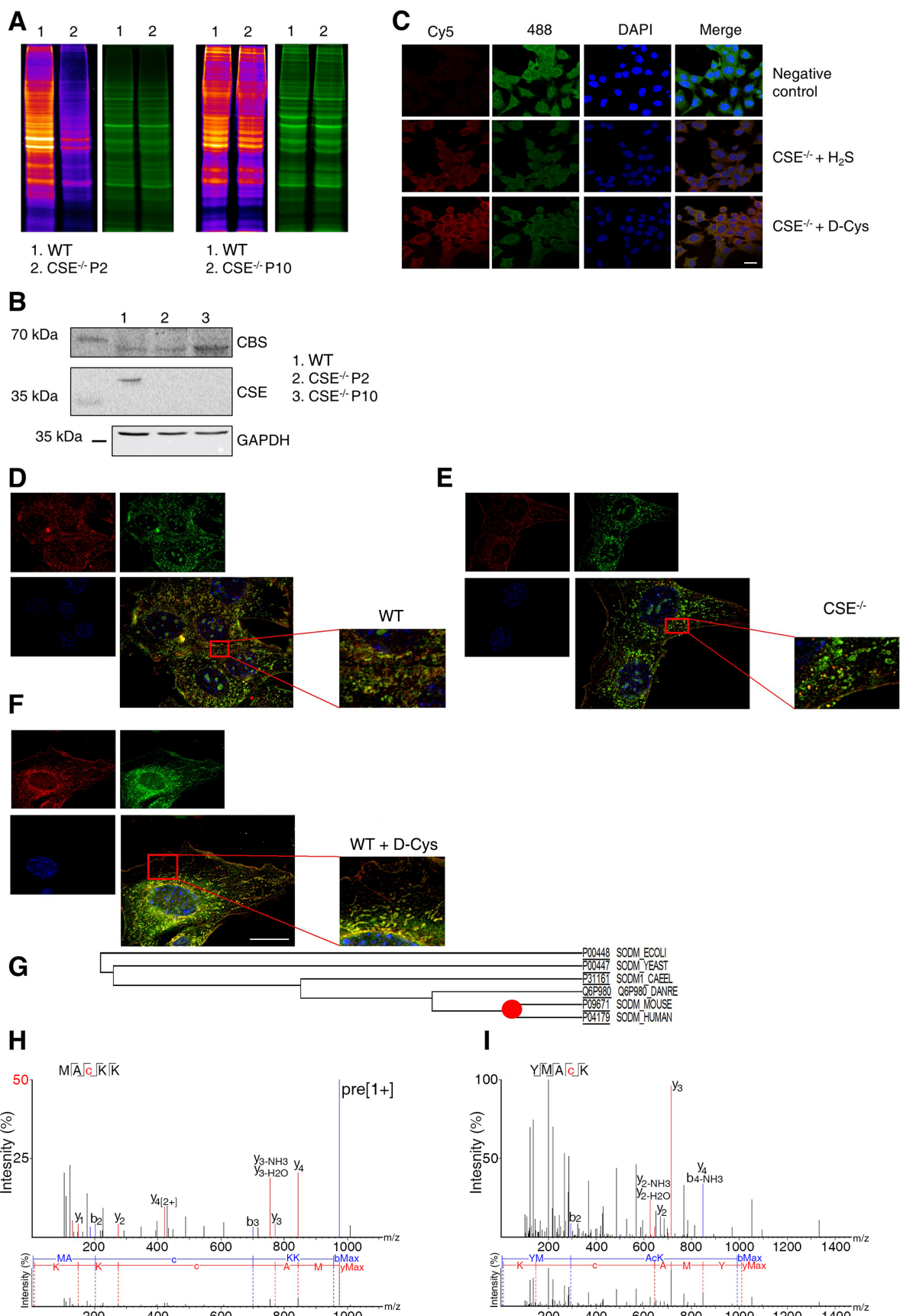
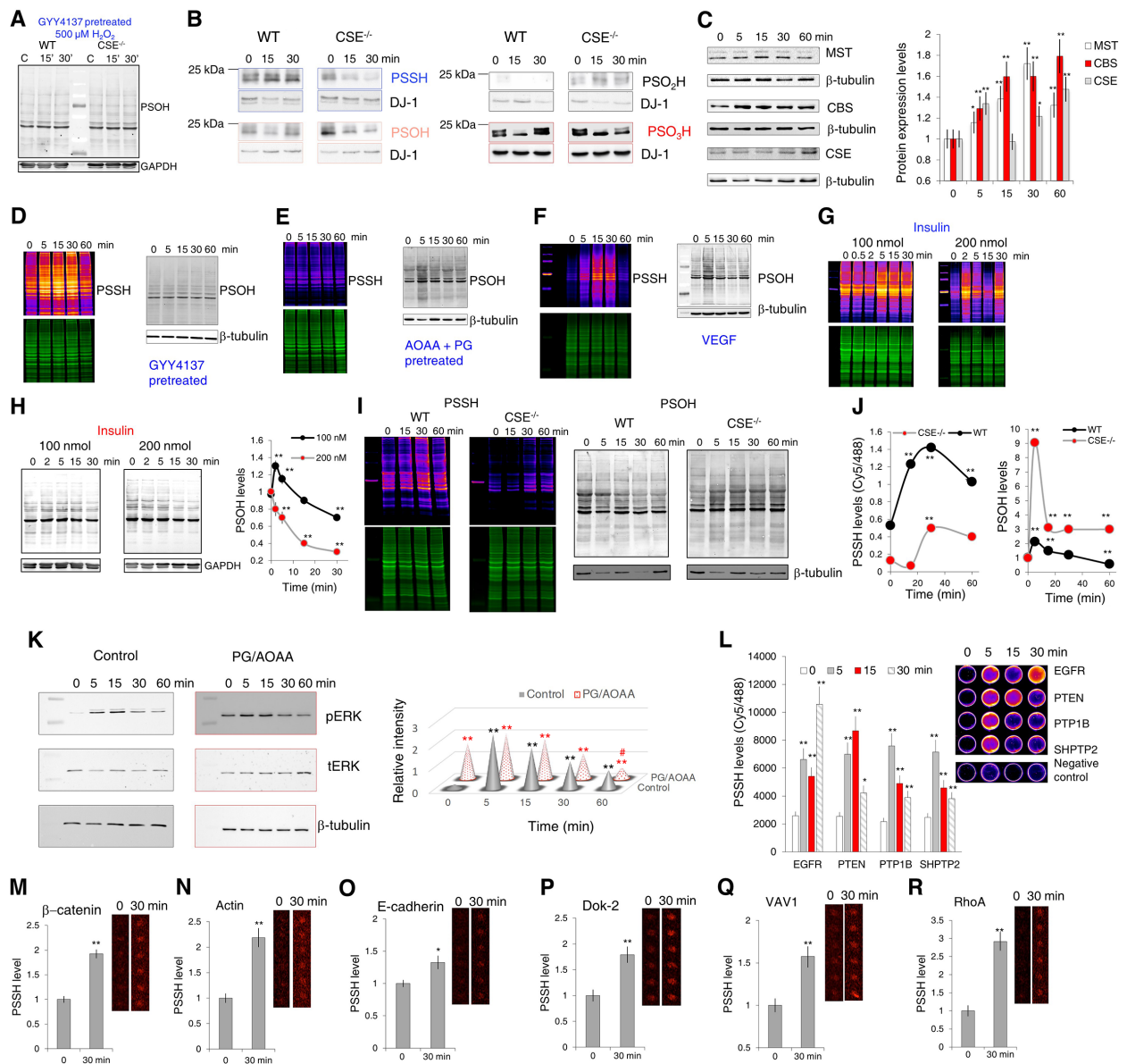


Figure S3. Broad applicability of dimedone switch method. Related to Figure 3.



**Figure S4. Protein persulfidation is an integral part of the cellular response to H<sub>2</sub>O<sub>2</sub> and RTK activation. Related to Figures 4 and 5.**

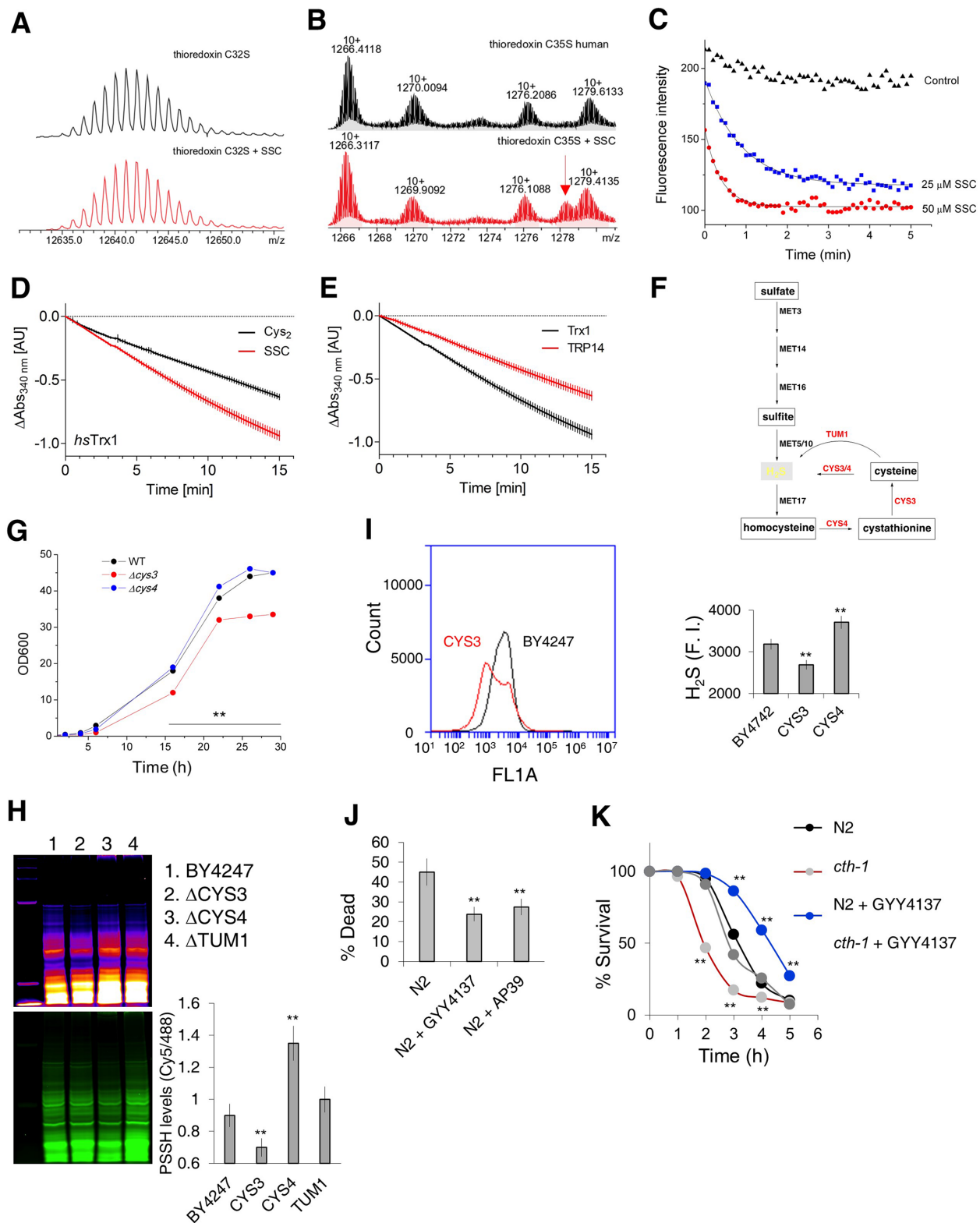


Figure S5. Trx-catalyzed reduction of *S*-sulfo-cysteine (SSC) and protection against ROS-induced death. Related to Figure 6

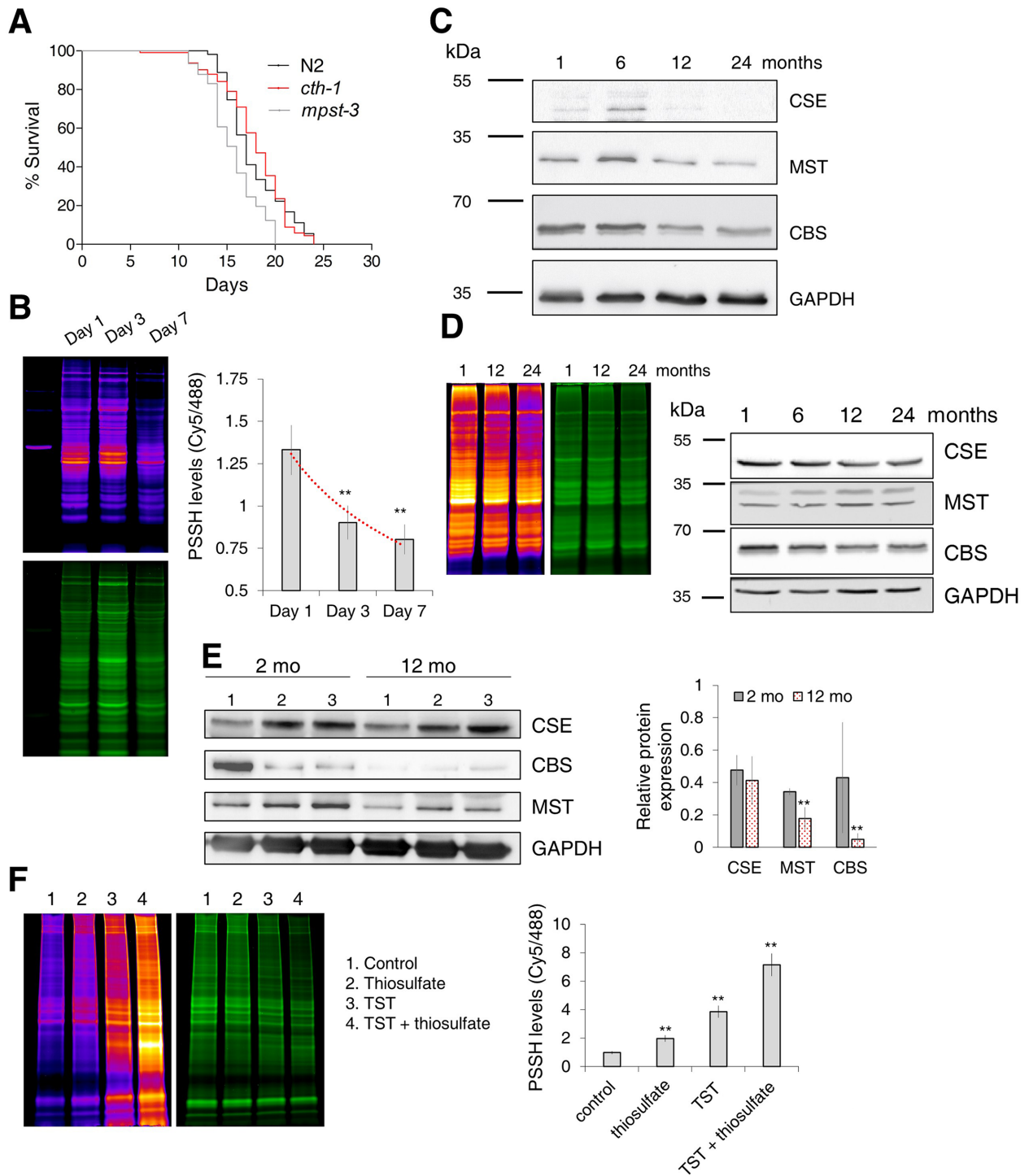


Figure S6. PSSH levels correlate with aging. Related to Figure 7.